Supplementary Material (ESI) for Chemical Communications
This journal is (c) The Royal Society of Chemistry 2007

1. Experimental Section

Synthesis Hydrochloric acid (36.0 wt%), titanium *n*-butyloxide ($Ti(OC_4H_9^n)_4$, Shanghai Chemical Co.), tetra-ethoxysilane ($Si(OC_2H_5)_4$,TEOS), Pluronic P123 (M_w=5800, containing 30.0 wt% ethylene glycol monomer, Sigma-Aldrich) and ethanol (>99.7%, Tianjin Chemical Co.) were all analytical grade and were used as received without further purification. In a typical synthesis of the silicic sol for electrospinning, 8.0 g (1.48 mmol) P123 was dissolved in 23.45 mL (18.76 g, 0.407 mol) absolute ethanol, then 3.76 mL (0.209 mol) distilled water and 0.6 mL 2.0 M HCl solution were added to the suspension. After P123 completely dissolved, 25.0 g (40.0 mmol) TEOS was added to the solution dropwise, and the mixture was transferred into a 250 mL three-neck flask under N_2 atmosphere and aged at 45 °C for 20 h to give a spinnable sol.

Characterization The rheology and visco-elasticity of the sol were measured on a RS75 rheometer (HAAKE Co.) at room temperature. The morphology and structure of the nanofibers were observed by use of a field emission scanning electron microscopy (FE-SEM, JSM-6700F). The low angle XRD (LA-XRD) patterns of the samples were recorded on an X-ray diffractometer (Rigaku D/Max 2200PC) with a graphite monochrometer using CuKα radiation (λ=0.15418 nm) in the range of 0.7-5° at room temperature while the voltage and electric current were held at 28 kV and 20 mA. The XRD patterns of the samples were applied to identify the phase of the core/shell nanofibers. The voltage and electric current were maintained at 40 kV and 20 mA (2θ=10-70^o). Thermal gravimetric (TG) analysis was employed to evaluate the weight loss of samples under an air flow of 20 $mL\cdot min^{-1}$ and heating rate of 20 $°C\cdot min^{-1}$ using a thermal analyzer (TGA/SDTA, 851^e METTLER). The infrared (IR) spectra were recorded on a Nicolet 5DX-FTIR spectrometer using KBr pellet method in the range of 400-4000 cm^{-1}. A high-resolution TEM (HR-TEM, GEOL-2010) was used to characterize the microstructure of the nanofibers. The samples were microtomed into thin slices and transferred onto carbon grids. The porous properties of samples were investigated using physical adsorption of N_2 at liquid-nitrogen temperature on an automatic volumetric sorption analyzer (Quantachrom SI). Prior to measurement, the samples were degassed at 300°C for 10 h. The specific surface area was determined according to the Brunauer-Emmett-Teller (BET) method in the relative pressure range of 0.05-1. The pore size distributions were obtained by analysis of the adsorption branch of the isotherm by the (Density Functional Theory) DFT methods.

Measurement of Photocatalytic Activity The photocatalytic activities of mesoporous composite nanofibers were characterized by the photo-oxidation of methylene blue (MB) and disperse red S-3GFL (DR) in aqueous solution. The photo- catalytic activities of mesoporous composite nanofibers were characterized by the photo-oxidation of methylene blue (MB) and disperse red S-3GFL (DR) in aqueous solution. A test quantity of 1.0 mg of composite nanofibers was added to 100.0 mL MB and DR mixed solution, in which MB and DR concentrations were both 5.0 mg/L, and the solution was irradiated with a 125 W high-pressure-mercury lamp (λ=320~400 nm, λ_{max}=365 nm) under stirring. The absorptions at 664 nm and 228 nm were applied to identify the MB and DR concentrations using a UV-vis spectrophotometer (Lambda 35, Perkin-Elmer) and their variations as a function of irradiation time were recorded against deionized water as a blank. As a comparison, the photocatalytic decomposition of separated MB and DR solutions with the same concentrations were also investigated.

2. Fig. S1. (a) TG curve of xerogel nanofibers, and (b) IR spectra of xerogel (1) and composite (2) nanofibers.

The TG curve (Fig. S1a) of the xerogel nanofibers shows three steps and a total weight loss of *ca*.70.0%. The first step of *ca*.7.7% from 60 to 150 °C could be attributed to the desorption of water, and the second significant weight loss of *ca*.60% between 150 °C to 400 °C was assigned to the decomposition of the template in the nanochannels of the composite nanofibers. From 400 °C to 600 °C, there was a weight loss of *ca*. 2.0%, which may result from loss of water from the hydroxyls and decomposition of a small amount of residual organic material. These results show that the organic template is removable from the nanofibers upon calcination at 400 °C. Above 400 °C, there is no significant weight loss, which indicates that the organic component is entirely decomposed.

The IR spectrum of the xerogel nanofibers (Fig. S1b1) shows a strong adsorption around 3400 cm^{-1}, which is assigned to the hydroxyls of water, P123 and Ti-OH, and the weak peak at 1720 cm^{-1} also indicates the presence of water. The adsorption peaks on 1520~1432 cm^{-1} are attributed to C-H vibrations of hydrocarbons in the xerogel nanofibers. After calcination at 400 °C (Fig. S1b, spectrum 2), the peaks in the range 1520~1432 cm^{-1} almost completely disappear, indicating the complete removal of P123, and absorptions around 530 cm^{-1} appear, which are attributed to the Ti-O vibrations of anatase TiO_2.

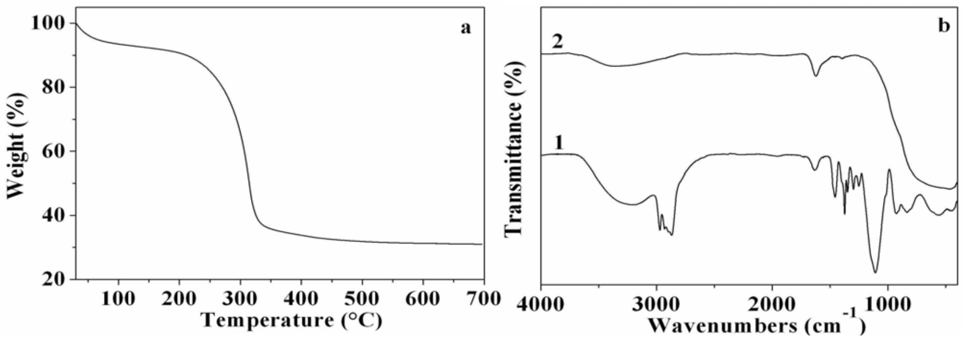

3. Fig. S2. LA-XRD patterns of xerogel (1) and composite (2) nanofibers. The inset in Fig. 1 is the XRD pattern of the composite nanofibers.

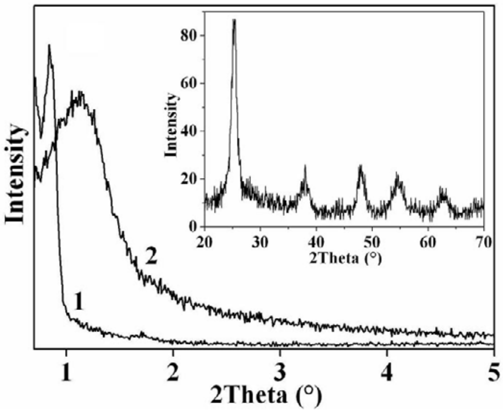

4. Fig. S3. HR-TEM images of the end of a typical core/shell nanofiber (a), TiO_2 core after dissolving the SiO_2 with hydrofluoric acid (18%) (b) and SiO_2 layers after dissolving the TiO_2 with concentrated H_2SO_4 (98%) (c).

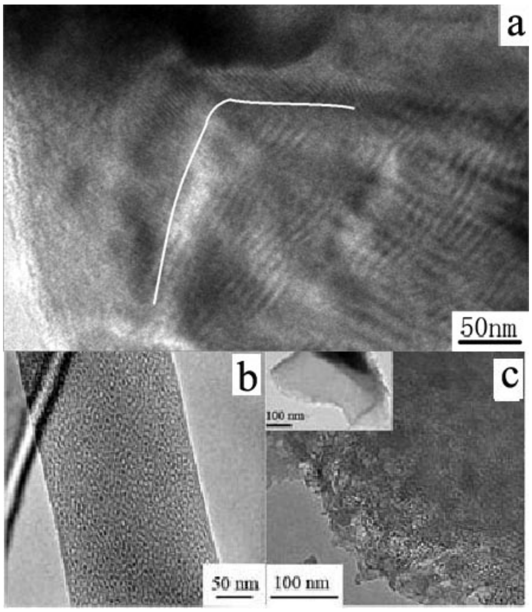

5. Fig. S4. EDS patterns of TiO_2/SiO_2 composite nanofibers (a), the surface of a single fiber (b), and the fiber after dissolving the SiO_2 with HF (c).

The major elements present in the composite nanofibers were determined by energy dispersive spectroscopy (EDS) (Fig. S4). The Ti contents for all nanofibers are much greater than silicon (Fig. S4a), which is consistent with the thinness of the mesoporous SiO_2 shell. As shown in Figure 4b, the silica peak (1.8 keV) only appears on the surface of the composite fiber. After dissolving the SiO_2 shell, only Ti element peaks appear (Fig. S4c), confirming the core/shell structure of the composite nanofibers.

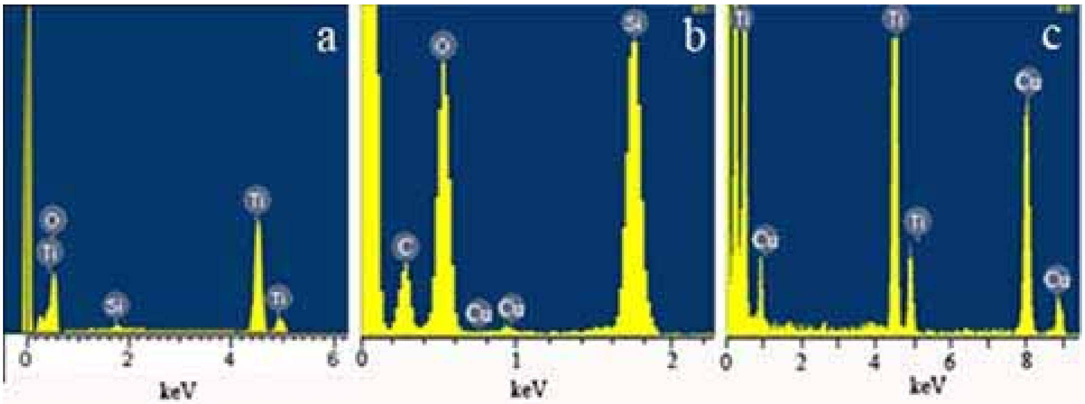

6. Fig. S5. UV-visible spectra of MB (a) and DR (b) solutions during photocatalysis with the TiO_2 core fibers after removing the SiO_2 shell.

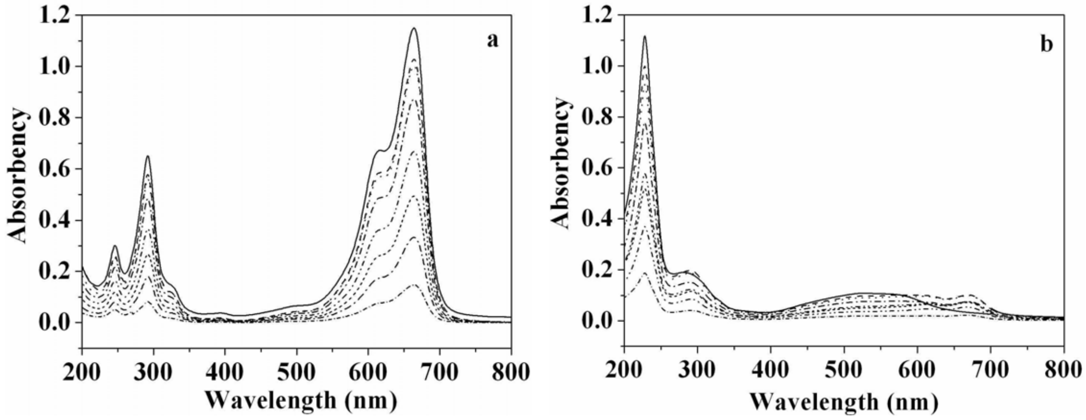

7. Fig. S6. Time courses for UV photo-degradation of DR (a) and MB (b) mixed solution, without photocatalyst, with mesoporous composite nanofibers (BET surface area: 353.7 m^2/g) and commercial

P25.

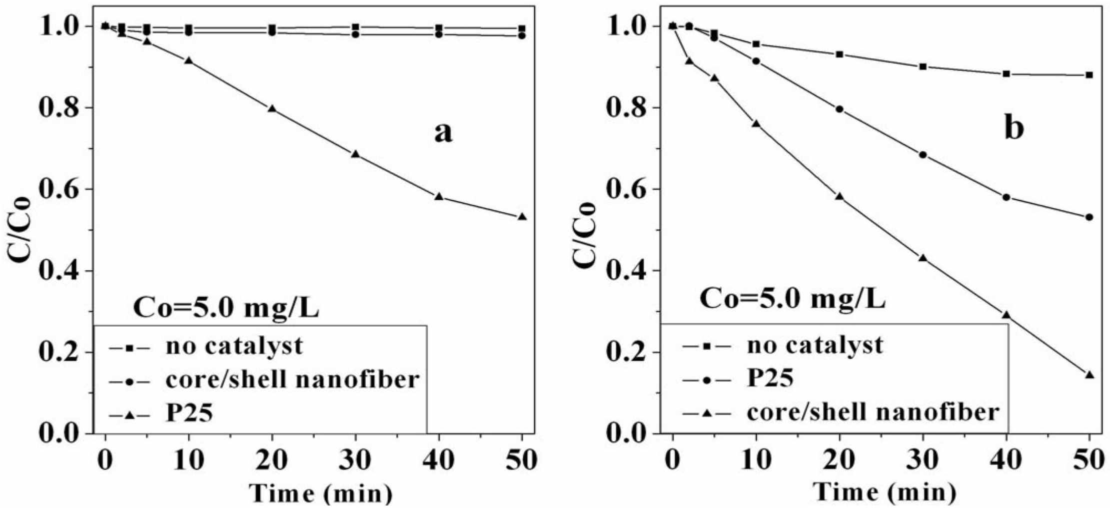

8. Fig. S7. Photographs of disperse red and methylene blue aqueous solution before and after filtration using a filter film with well-proportioned 0.2 μm pores (a), and the color difference between inner and outer solutions after dialysis against deionized water for 5 h (b).

To further validate the difference of solubility and crystal size in the aqueous solution for these dissimilar type of dyestuffs,[1-2] filter film with well-proportioned 0.2 μm pores and a dialysis bag (Spectra/Por MWco=14000, Beijing Jingkehongda Biotechnology Co., Ltd) were used. As shown in Fig. S7a, when the two different dyes with the same concentration were filtered using the super-fine filter film, the disperse red was eliminated. However, the methylene blue molecules were smaller than the pores, so the filter solution remained a deep blue. Similarly, the semi-permeable dialysis bags (Fig. S7b) filled with these two dyes were put in a beaker containing the same volume of water. After 5 h, it was found that the water outside of the semi-permeable dialysis bag containing disperse red solution remained colorless because disperse red particles were too large to diffuse out. In contrast, the color of the inner and outer solutions of methylene blue were almost the same. This result accords with the photocatalytic experiments,[3-4] which demonstrate that the disperse red particles could not adsorb to the anatase TiO_2 core of the mesoporous core/shell fibers, and, consequently, was not decomposed.

9. Fig. S8. Photographs of the color difference between inner and outer active yellow K-4G (AY) solutions after dialysis against deionized water for 5 h (a), AY aqueous solution before and after filtration using a filter film with well-proportioned 0.2 μm pores (b); UV-visible spectra of only AY solution (c), AY and DR mixed solution (d) during photocatalysis with the TiO_2 core fibers after removing the SiO_2 shell; Time courses for UV photo-degradation of AY (e) in the AY and DR mixed solution, without photocatalyst, with mesoporous composite nanofibers (BET surface area: 353.7 m^2/g) and commercial P25.

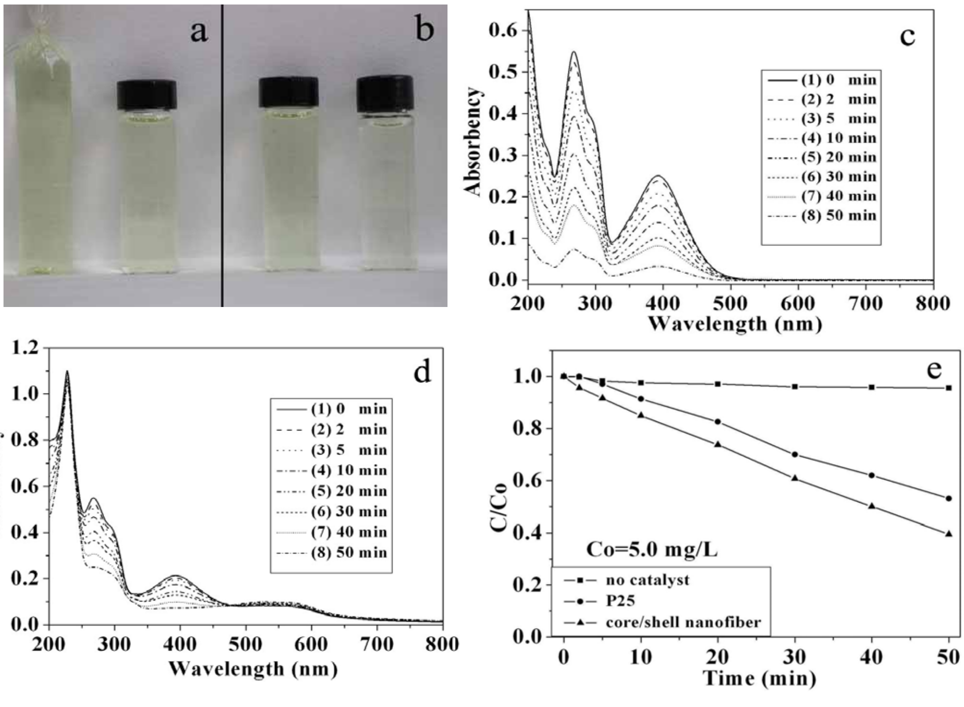

Yan et al. (X. Yan, T. Ohno, K. Nishijima, R. Abe and B. Ohtani, *Chem. Phys. Lett.,* 2006, ***429***, 606) mentioned that the methylene blue (MB) maybe is not an appropriate photocatalytic substrate for a given semiconductor material with visible-light photocatalytic activity because MB can absorb in the visible region. In our experiment, a 125 W high-pressure-mercury lamp (λ=320~400 nm, λ_{max}=365 nm) was used to produce ultraviolet radiation, which is different from the 300 W Xenon lamp in their article, so the visible-light induced decomposition of MB may be ignored. To avoid the adsorbent difference of these two dyes, active yellow K-4G (AY) with only UV adsorption was also selected to test the composite nanofibers' selective photocatalytic property instead of MB dye.

Because the active yellow K-4G (AY) is a kind of water-soluble dye, so in the aqueous solution, the AY molecules can also easily cross the channels to be decomposed on the TiO_2 surface because of their small size. This can be proved by the same method as shown in Fig. S7. As shown in Fig. S8a, the semi-permeable dialysis bags filled with active yellow dye was put in a beaker containing the same volume of water. After 5 h, it was found that the water outside of the semi-permeable dialysis bag containing AY solution became yellow similar with the inner color. The AY molecules were smaller than the 0.2 μm pores of the super filter film, so the filter solution remained yellow (Fig. S8b).

Using the nanofibrous cores after dissolution of SiO_2 as photo-catalyst, the absorptions of both AY (Fig. S8c) and DR (Fig. S5b) almost completely disappear after irradiation for 50 min. While using the composite nanofibers as the photocatalyst, the selective photocatalytic property is obvious, and only the absorption peaks of AY disappear at 268 nm and the DR absorption at 228 nm remains unchanged (Fig. S8d). Fig. S8e shows the photo-catalytic activities of the mesoporous composite nanofibers. In the absence of catalyst, AY hardly decompose under UV light irradiation, in the presence of the composite nanofibers the photo-degradation rate of AY is faster than that by P25.

References

(1) J. Oh, H. Imai and H. Hirashima, *Chem. Mater.* 1998, ***10,*** 1582.

(2) (a) E. Beyers, P. Cool and E. F. Vansant, *J. Phys. Chem. B* 2005, ***109***, 10081; (b) C. Zhang and Y. Zhu, *Chem. Mater*. 2005, ***17***, 3537; (c) J. C. Yu, W. Ho, J. Yu, S. K. Hark and K. Iu, *Langmuir* 2003, ***19***, 3889; (d) T. Sreethawong, Y. Suzuki and S. Yoshikawa, *J. Solid State Chem*. 2005, ***178***, 329.

(3) (a) I. M. Butterfield, P. A. Christensen and A. Hamnett, *J. Appl. Electrochem*. 1997, ***27***, 385; (b) J. Chen,

W. H. Rulkens and H. Bruning, *Water Sci. Technol.* 1997, ***35***, 231; (c) I. Sopyan, M. Watanabe, S. Murasawa, K. Hashimoto and A. Fujishima, *J. Photochem. Photobiol. A: Chem.* 1996, ***98***, 79; (d) Y. Zhu, L. Zhang, W. Yao and L. Cao, *Appl. Surf. Sci.* 2000, ***158***, 32.

(4) (a) C. E. Webster, R. S. Drago and M. C. Zerner, *J. Phys. Chem. B* 1999, ***103,*** 1242; (b) J. Xi, S. Miao and X. Tang, *Macromolecules* 2004, ***37,*** 8592; (c) C. D. Chudasama, J. Sebastian and R. V. Jasra, *Ind. Eng. Chem. Res.* 2005, ***44,*** 1780.